




## BRIEF REPORT OPEN ACCESS

# Comparative DNA Methylation Profiling of Human and Murine ALK-Positive B-Cell Neoplasms

Selina Glaser<sup>1</sup>  | Rabea Wagener<sup>1,2</sup> | Shannon K. Harkins<sup>3</sup> | Claudia Voena<sup>4</sup> | Susanne Bens<sup>1</sup> | Wolfram Klapper<sup>5</sup>  | Camille Laurent<sup>6</sup> | Stephan Mathas<sup>7,8,9</sup> | Meiqi Ren<sup>10</sup> | Sandrine Sander<sup>10,11</sup> | Charlotte Schnaudt-Mastrangelo<sup>1</sup> | Wilhelm Wöbmann<sup>12</sup>  | Luc Xerri<sup>13</sup> | Ole Ammerpohl<sup>1,2,14,15</sup> | Andrew D. Zelenetz<sup>16</sup> | Abner Louissaint Jr<sup>3</sup> | Roberto Chiarle<sup>4,17,18</sup> | Reiner Siebert<sup>1,2,15</sup>

<sup>1</sup>Institute of Human Genetics, Ulm University and Ulm University Medical Center, Ulm, Germany | <sup>2</sup>Institute of Human Genetics, Christian-Albrechts-University Kiel, Kiel, Germany | <sup>3</sup>Department of Pathology, Massachusetts General Hospital and Harvard Medical School, Boston, Massachusetts, USA | <sup>4</sup>Department of Molecular Biotechnology and Health Sciences, University of Torino, Torino, Italy | <sup>5</sup>Hematopathology Section, Institute of Pathology, Christian-Albrechts-University, Kiel, Germany | <sup>6</sup>Department of Pathology, Institut Universitaire du Cancer de Toulouse-OncoPole, and Laboratoire d'Excellence Toulouse Cancer, Centre de Recherche en Cancérologie de Toulouse INSERM U1037, Toulouse, France | <sup>7</sup>Max-Delbrück-Center for Molecular Medicine in the Helmholtz Association (MDC), Group Biology of Malignant Lymphomas, Berlin, Germany | <sup>8</sup>Charité-Universitätsmedizin Berlin, Hematology, Oncology and Tumor Immunology, Corporate Member of Freie Universität Berlin and Humboldt-Universität Zu Berlin, Berlin, Germany | <sup>9</sup>Experimental and Clinical Research Center (ECRC), a Joint Cooperation Between the MDC and the Charité, Berlin, Germany | <sup>10</sup>Division Adaptive Immunity and Lymphoma, German Cancer Research Center (DKFZ) Heidelberg, Heidelberg, Germany | <sup>11</sup>Comprehensive Cancer Center (CCC) Mecklenburg-Vorpommern, University Medicine Greifswald, Greifswald, Germany | <sup>12</sup>Pediatric Hematology and Oncology and NHL-BFM Study Center, Medical Center Hamburg-Eppendorf, Hamburg, Germany | <sup>13</sup>Department of Pathology, Institut Paoli-Calmettes, Centre de Recherche en Cancérologie de Marseille, Aix-Marseille University, Marseille, France | <sup>14</sup>Airway Research Center North, Member of the German Center for Lung Research (DZL), Grosshansdorf, Germany | <sup>15</sup>German Center for Child and Adolescent Health (DZKJ), Partner Site Ulm, Ulm, Germany | <sup>16</sup>Lymphoma Service, Department of Medicine, Memorial Sloan Kettering Cancer Center, New York, New York, USA | <sup>17</sup>Department of Pathology, Boston Children's Hospital, Harvard Medical School, Boston, Massachusetts, USA | <sup>18</sup>Hematopathology Division, IRCCS Istituto Europeo di Oncologia, Milan, Italy

**Correspondence:** Reiner Siebert ([reiner.siebert@uni-ulm.de](mailto:reiner.siebert@uni-ulm.de))

**Received:** 24 February 2025 | **Revised:** 28 May 2025 | **Accepted:** 19 June 2025

**Funding:** This study has been supported by grants from the German Research Foundation (DFG) in the framework of the Collaborative Research Centres SFB 1074 to R.S. and SFB 1530 to S.S. This work was supported by NIH/NCI R01 CA196703-01 to R.C.

**Keywords:** ALK-positive LBCLs | DNA methylation | transgenic mouse model

## ABSTRACT

Structural genomic variants leading to anaplastic lymphoma kinase (ALK) gene fusions and aberrant expression of the ALK tyrosine kinase are the hallmark of subtypes of T- and B-lineage neoplasms, namely ALK-positive anaplastic large lymphoma (ALCL) and ALK-positive large B-cell lymphoma (LBCL). The latter is a rare aggressive lymphoma, which has been initially identified as a variant of diffuse LBCL (DLBCL) with plasmablastic features. Here, we performed comparative DNA methylation profiling of human and murine ALK-positive B-cell neoplasms. Array-based DNA methylation data from ALK-positive LBCL samples of eight patients were compared to that of DLBCL ( $n = 75$ ), multiple myeloma (MM,  $n = 24$ ), ALK-positive ALCL ( $n = 12$ ) and normal B-cell populations ( $n = 93$ ). ALK-positive LBCLs share a distinct DNA methylation signature similar to that of MM, characterized by lower global DNA methylation levels compared to DLBCLs and normal B-cell populations. DNA methylation alterations in ALK-positive LBCL were predominantly located in heterochromatic and polycomb-repressed regions. The epigenetic age and relative proliferative history of ALK-positive LBCL were intermediate between MM and DLBCL. B-cell neoplasms in *NPM::ALK* transgenic mice showed a similar hypomethylated signature when compared to normal murine B cells. Cross-species comparison indicated conservation of chromatin states and pathways affected by hypomethylation. Together, the

This is an open access article under the terms of the [Creative Commons Attribution](https://creativecommons.org/licenses/by/4.0/) License, which permits use, distribution and reproduction in any medium, provided the original work is properly cited.

© 2025 The Author(s). Genes, Chromosomes and Cancer published by Wiley Periodicals LLC.

findings suggest that in line with their phenotypical appearance human and murine ALK-positive B-cell lymphomas share an epigenetic profile more closely resembling that of plasma cell neoplasias than that of DLBCLs.

## 1 | Introduction

Anaplastic lymphoma kinase (ALK)-positive large B-cell lymphoma (LBCL) is a mature B-cell lymphoma, which based on its typical morphology, has been assigned as a definitive entity to the group of LBCL in the Fifth Edition of the WHO Classification of haematolymphoid tumors [1]. It is a diffuse, monomorphic neoplasm of large B cells with a plasmablastic immunophenotype, negative for typical T- and B-cell markers and CD30, but positive for plasma cell markers such as MUM1, CD38, and CD138 [1, 2]. The most common ALK fusion partner is clathrin heavy chain (CLTC), leading to activation of the STAT3/STAT5, PI3K/AKT, PLCG2, and ERK pathways due to constitutive ALK tyrosine kinase activity [1, 2].

Despite the rarity of ALK-positive LBCL, recent reviews report a poor prognosis with a 5-year survival rate of only 28%, and a male predominance with most cases diagnosed in individuals under 40 years, which contrasts with typical LBCLs, which usually affect older adults [2, 3]. Nevertheless, ALK inhibitors have been proven effective in ALK-positive LBCL patients with subsequent marrow transplantation [4–6].

Originally, ALK fusions were first discovered in anaplastic large cell lymphoma (ALCL), which is a distinct T-cell lymphoma characterized by strong CD30 expression and frequent *NPM::ALK* fusions [1, 7]. Interestingly, different *NPM::ALK* mouse models, besides T-cell lymphomas, also develop a spectrum of clonal B-cell neoplasms, indicating that ALK fusion is also an efficient driver in B-cell lymphomagenesis [8, 9].

To provide further insights into the pathogenesis of ALK-positive B-cell neoplasms, we performed comparative DNA methylation profiling of human and murine ALK-positive B-cell neoplasms. Comparison to the DNA methylation profiles of DLBCL, multiple myeloma (MM), and ALK-positive ALCL suggests an ALK-positive LBCL group with plasma cell neoplasms in line with its phenotype.

## 2 | Material and Methods

### 2.1 | Human Lymphoma and Control Samples

The study cohort included formalin-fixed paraffin-embedded (FFPE) lymphoma samples from seven patients with ALK-positive LBCL (Table S1), one of which was from a relapse after Crizotinib treatment. A patient-derived xenograft (PDX) model from this relapse sample was also profiled [5]. Additionally, the ALK-positive LBCL cell line LM1, derived from the bone marrow of a 13-year-old girl with a systemic relapse of *CLTC::ALK*-positive DLBCL, was studied [4]. The study was approved by the Ethics Committee of the Medical Faculty of the Christian-Albrechts-Universität Kiel (D447/10, Amendment 2.11.2015).

For comparison, published DNA methylation data of 75 DLBCLs [10], 24 MMs [11], and 12 ALK-positive ALCL [12], and various normal B-cell populations ( $n = 93$ ) were included (Table S2) [13–16].

### 2.2 | Murine Lymphoma and Control Samples

ALK-positive B-cell neoplasms named herein *NPM::ALK* positive plasmacytomas were obtained from *NPM::ALK* transgenic mice (C57BL/6J) previously described by Chiarle et al. [8]. In total, FFPE tissue sections from six *NPM::ALK* plasmacytomas were included, and DNA methylation profiles were generated in duplicate for each sample. Animals were housed and maintained in the Animal Facility of the Department of Molecular Biotechnology and Health Sciences of the University of Torino. Animal experiments were performed under protocols approved by the Italian Ministry of Health for the University of Torino (approval n. n 560/2022-PR).

For comparison, flow-sorted germinal center B cells (gcBCs) were collected from three Rag2<sup>cg<sup>KO</sup></sup> mice, whose lymphoid system had been successfully reconstituted after transplantation of bone marrow cells isolated from *Cy1-cre*, *R26Stop<sup>FL</sup>eYFP* animals [17]. Viable splenic gcBCs were sorted at day 10 post-immunization (using sheep red blood cells) based on CD19+, B220+, CD38 low, FAS high, and YFP+ markers (Table S3). Animal care and procedures for the latter mice were approved by the Regierungspräsidium Karlsruhe (G-119/17).

### 2.3 | DNA Methylation Analysis by Illumina Methylation Arrays

For human samples, in-house generated and publicly available DNA methylation data were evaluated from both Infinium HumanMethylation450 (450k) or Infinium MethylationEPIC (EPIC) BeadChips (Illumina Inc., San Diego, CA, USA). Raw intensity signals were normalized (intrinsic controls, no background correction) with the minfi package, including 441 870 CpGs [18].

Raw DNA methylation values of murine samples were custom-generated by a service provider (Life & Brain GmbH, Bonn, Germany) using the Infinium Mouse Methylation BeadChip (Illumina Inc., San Diego, CA, USA). Raw intensity signals were normalized with GenomeStudio (v2011.1; methylation module 1.9.0; Illumina Inc., San Diego, CA, USA) applying default settings and internal normalization controls, resulting in 266 961 CpGs. For details refer to Data S2.

### 2.4 | Segmentation of Chromatin States in Humans and in Mice

Chromatin states in human gcBCs were based on the data from Kretzmer et al., with raw sequencing data publicly available from the European Nucleotide Archive (ENA) [16].

For murine data, publicly available ChIP-Seq data for H3K27ac, H3K27me3, H3K4me1, H3K4me3, and H3K36me3 marks from the spleen and thymus of 8-week-old mice were sourced from ENCODE (Lab: Bing Ren, UCSD, Tables S4 and S5) [19]. For details, refer to Data S2.

## 2.5 | Bioinformatic and Statistical Analyses

All statistical analyses were performed in R (version 4.3.0). Differentially methylated loci were identified using the limma package (version 3.58.1), with multiple comparison correction via the Benjamini-Hochberg method (FDR) [20]. CpGs with  $FDR < 0.01$  and mean  $|\Delta\beta| > 0.3$  were considered significantly different. To identify genes affected by hyper- or hypomethylation in both species, the mouse gene names were converted into human gene names using the online tool Biomart. Fisher's exact test was applied to categorical variables to calculate odds ratios and  $p$  values, while the Wilcoxon rank sum test was used for pairwise comparisons of continuous variables. Multiple comparisons were corrected using Benjamini-Hochberg.

## 3 | Results

### 3.1 | The DNA Methylation Profile Groups Human ALK-Positive LBCL Apart From DLBCL

We investigated DNA methylation data obtained by Illumina BeadChip arrays from seven ALK-positive LBCLs, a PDX model derived from one of these tumors and the ALK-positive LBCL cell line LM1. Considering also the LM1 cell line [4], the median age at diagnosis of all eight patients was 43 years (range: 9–68 years), with six cases being male. The ALK fusion partner has been proven to be CLTC in five cases, while also the others showed the granular-cytoplasmic immunohistochemical pattern of ALK expression typical for the same fusion.

In its initial description, ALK-positive LBCL was considered as variant of DLBCL [3, 21, 22]. Therefore, and because of its LBCL morphology, we initially compared the DNA methylation profiles of the ALK-positive LBCL to that of 75 DLBCLs. Hierarchical clustering of 441 870 CpGs distinctly separated ALK-positive LBCL and LM1 from DLBCL, with two DLBCL cases clustering within the ALK-positive LBCL branch (Figure 1A).

### 3.2 | The DNA Methylation Profile of Human ALK-Positive LBCL Shows Similarities to Plasma Cell Neoplasias

Having shown that ALK-positive LBCL segregate apart of DLBCL we asked whether the plasmablastic features or constitutive ALK-signaling might be reflected by the methylation profile. Therefore, we compared the methylation profile of the ALK-positive LBCL with the one of 24MMs, 12 ALK-positive ALCLs and non-neoplastic B-cell populations ( $n = 93$ ).

UMAP analysis using data from all 441 870 CpGs across all neoplasms revealed a clear separation of ALK-positive LBCL from DLBCL, ALK-positive ALCL and also from MM (Figure S1). ALK-positive ALCLs, except one case, clustered clearly apart from the ALK-positive LBCL. Therefore, and taking into account their T-cell origin, they were not further considered in the subsequent analyses.

Focusing on the 10 000 most variable CpGs (mvCpGs) within the neoplastic B-cell samples, two distinct clusters emerged: one containing the ALK-positive LBCL and MM, and the other comprising all DLBCLs (Figure 1B and S2). Moreover, we investigated the median DNA methylation levels across the 441 870 CpGs. This demonstrated a prevalent low median DNA methylation in MM (0.26 [0.13–0.41]) and in ALK-positive LBCL (0.39 [0.26–0.46]). Conversely, DLBCL, independent of their cell of origin gene expression signature (Figure S3), along with normal B-cell populations, demonstrated median DNA methylation levels ranging from 0.28 to 0.72 (Figure 1C). Notably, the two DLBCL cases clustering within the ALK-positive LBCL branch (Figure 1A) showed also a low median DNA methylation in the range of that of ALK-positive LBCL (annotated in Figure 1C).

Next, we investigated the epigenetic age by the Horvath clock and evaluated the relative proliferative history utilizing the epigenetically-derived cumulative mitotic clock (epiCMIT), leading to congruent findings. The highest median epigenetic age and proliferation history was observed in MM (median [range]: age: 102 [53–170] years; proliferation: 0.8 [0.7–0.9]) followed by comparable values between ALK-positive LBCL (age: 68 [43–103] years; proliferation: 0.6 [0.5–0.7]) and DLBCL (age: 76 [19–128] years; proliferation: 0.6 [0.4–0.9]), although in all entities high variances were observed (Figure S4A,B). Decreasing median DNA methylation levels in tumor and normal B cells show a strong correlation with relative proliferation history ( $R = -0.88$ ,  $p$  value  $< 0.001$ ) and epigenetic age ( $R = -0.73$ ,  $p$  value  $< 0.01$ ) (Figure S4C,D).

Given the distinct separation of ALK-positive LBCL and MM from DLBCL, we further analyzed the 10 000 mvCpGs using K-means clustering, identifying two clusters: Cluster 1 (4861 CpGs) and Cluster 2 (5139 CpGs) (Figure 1D). Both clusters (all 10 000 mvCpGs) showed low DNA methylation levels in ALK-positive LBCLs (median [range]: 0.42 [0.35–0.50]) and MM (median [range]: 0.17 [0.07–0.33]), with slightly higher DNA methylation levels in Cluster 2 for ALK-positive LBCLs (median [range]: 0.49 [0.42–0.59]) compared to MM (median [range]: 0.25 [0.09–0.40]; adj.  $p$  value = 0.0022). Although DLBCLs showed somewhat higher DNA methylation levels in Cluster 1 (median [range]: 0.51 [0.05–0.86]), overall, Cluster 2 exhibited high DNA methylation levels (median [range]: 0.84 [0.51–0.89]), similar to normal B-cell populations (median [range]: 0.90 [0.82–0.92]) (Figure 1E). Consistent with these findings, differential DNA methylation analysis between ALK-positive LBCL and MM versus DLBCL identified a widespread hypomethylated signature ( $FDR < 0.01$  and mean  $|\Delta\beta| > 0.4$ , 9198 CpGs) in heterochromatic regions (Figure S5), with MM showing a more pronounced hypomethylation compared to ALK-positive LBCL (Figure S6).

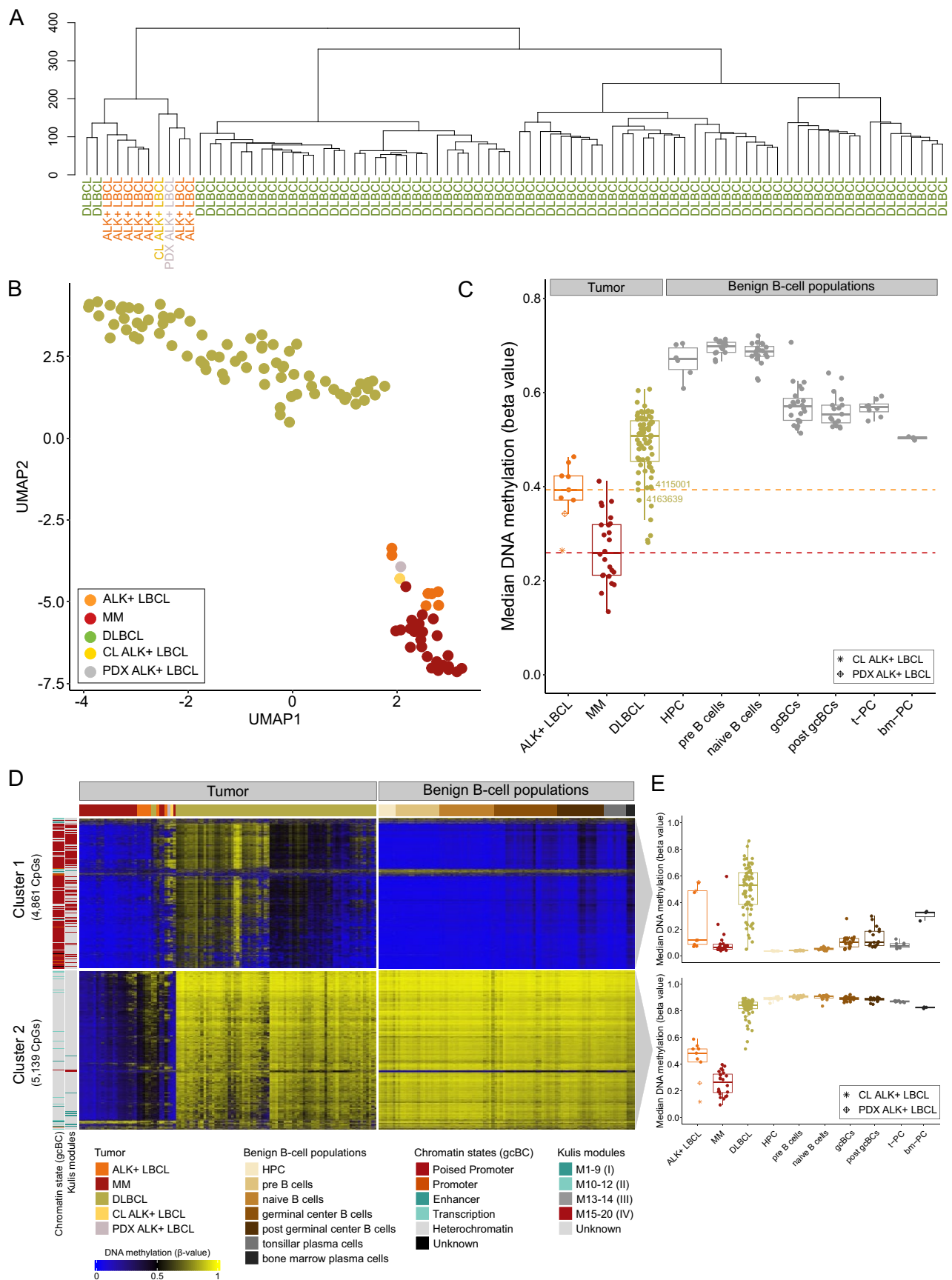


FIGURE 1 | Legend on next page.

### 3.3 | Functional Analysis of the 10 000 Most Variable CpGs

Next, we mapped the CpGs within the two clusters to chromatin states defined in gcBCs, as well as sets of CpGs known to undergo dynamic DNA methylation during B-cell differentiation (Kulis modules M1-M20) (Figure S7 and Table S6) [14]. CpGs in Cluster 2, which showed low DNA methylation in MM and ALK-positive LBCLs but high methylation levels in DLBCL and normal B-cell populations, were predominantly localized in heterochromatin (OR=13.0,  $p$  value<0.001) and associated with Kulis module M9 (OR=4.8,  $p$  value<0.001). Conversely, CpGs within Cluster 1 were mainly localized within polycomb-repressed regions (OR=24.6,  $p$  value<0.001), CpG islands (OR=9.9,  $p$  value<0.001) and assigned to modules M19 (OR=2.4,  $p$  value<0.001) and M20 (OR=29.1,  $p$  value<0.001).

In conclusion, DNA methylation profiles of ALK-positive LBCL exhibit similarity to MM, marked by DNA methylation alterations in non-functional genomic elements such as heterochromatic and polycomb-repressed regions.

### 3.4 | Hypomethylated Epiphenotype in B-Cell Neoplasms of *NPM::ALK* Transgenic Mice

In order to investigate whether B-cell tumor induction by the *NPM::ALK* transgene in mice enforces similar DNA methylation changes as seen in human ALK-positive LBCL, we evaluated the DNA methylation levels across the 266961 CpG sites in duplicates of six samples of B-cell neoplasias from *NPM::ALK* transgenic mice compared to three samples from sorted cells with a gcBC phenotype. Consistent with our findings in human ALK-positive LBCLs, the B-cell neoplasms of the *NPM::ALK* transgenic mice showed a significantly lower DNA methylation (median [range]: 0.42 [0.26–0.45]) than the benign B cells (median [range]: 0.66 [0.64–0.66]; Wilcoxon rank sum test:  $p=0.024$ ) (Figure 2A). Examination of 10000 mvCpGs demonstrated clear differentiation between tumor and normal B cells in a PCA (PC1: 90% variance) (Figure 2B). Moreover, a predominantly low methylated signature (9167 of the 10000 CpGs) was observed within the tumors of the *NPM::ALK* transgenic mice (Figure 2C), similar to the hypomethylation seen in ALK-positive LBCL.

### 3.5 | Cross-Species DNA Methylation Analysis of ALK-Positive B-Cell Neoplasms

As similar DNA methylation patterns were seen in human and murine ALK-positive B-cell neoplasms, we aimed for a

cross-species epigenetic comparison to identify potential conserved mechanisms of lymphomagenesis. To this end, significantly differentially methylated CpGs (DMCs) between tumor and non-malignant gcBCs as control group were identified from the samples of both species (FDR < 0.01, mean  $|\Delta\beta| > 0.3$ ). Similar numbers of DMCs were detected in both human and mice, namely 54006 CpGs in human and 54407 CpGs in mice (Tables S7 and S8). Consistent with our previous results, a predominantly hypomethylated pattern was observed in the ALK-positive neoplasms as compared to controls in both species (human: 49426 CpGs; mice: 51909 CpGs, Figure S8). Chromatin mapping unveiled that hypomethylated DMCs were predominantly localized within heterochromatic regions (OR mouse: 8.0, adj.  $p$  value<0.001; OR human: 13.9, adj.  $p$  value<0.001), whereas hypermethylated DMCs were localized in promoter (OR mouse: 2.5, adj.  $p$  value<0.001; OR human: 1.4, adj.  $p$  value<0.001) and enhancer regions (OR mouse: 7.7, adj.  $p$  value<0.001; OR human: 5.6, adj.  $p$  value<0.001) (Figure 2D and Table S9). Tumors from both species share 3829 genes with hypomethylated DMCs (33%) and 324 genes with hypermethylated DMCs (12%) in ALK-positive B-cell neoplasms (Figure 2E). From these, 177 hypomethylated and 215 hypermethylated genes were found to be affected by DMCs in regulatory regions, including promoters and enhancers, and were subsequently used for pathway enrichment analysis. Enrichment analysis revealed that hypermethylated genes were enriched in immune system-related pathways, while hypomethylated genes were primarily enriched in signal transduction pathways (Figure 2F and Table S10).

## 4 | Discussion

Our comprehensive DNA methylation profiling of human and murine ALK-positive LBCLs, human DLBCL, MM, and ALK-positive ALCL reveals that ALK-positive LBCL shares several DNA methylation features with MM. This is consistent with the lymphoma's plasmablast-like morphology and expression of plasma cell markers such as CD138, VS38C, and MUM1, the latter being a key plasma cell differentiation factor encoded by the *IRF4* gene [2, 23]. These findings suggest that ALK-positive LBCL is more closely aligned with plasma cell neoplasms than DLBCL, although the slightly higher DNA methylation levels in ALK-positive LBCL compared to MM suggest a cellular counterpart that is transitioning toward plasma cells but not yet fully differentiated. This observation indicates that the normal cellular counterpart may influence the methylation profile, but not the oncogenic driver ALK.

Both ALK-positive LBCL and MM exhibit global DNA hypomethylation compared to DLBCL and normal B-cell

**FIGURE 1** | DNA methylation profiling of human ALK-positive LBCLs. (A): Hierarchical clustering (ward.d2) dendrogram of 441 870 CpGs. The analysis includes seven ALK-positive LBCL cases, the LM1 cell line (CL), the patient-derived xenograft (PDX) model, and 75 DLBCLs. Cluster relationships highlight the epigenetic similarities and differences across these samples. (B) UMAP analysis of B-cell lymphomas based on the 10000 most variable CpGs (20 neighbors). (C) Median DNA methylation of various lymphomas and benign B-cell populations across the 441870 CpGs entered downstream analyses. (D) Heatmap displaying the 10000 most variable CpGs across ALK-positive LBCLs, DLBCL, and multiple myeloma (MM). Rows represent CpGs and columns represent samples. Tumor samples are clustered using hierarchical clustering (ward.d, dendrogram are not shown). Benign B-cell populations are only displayed and ordered according differentiation status. K-means clustering on the CpGs revealed two clusters (Cluster 1: 4861 CpGs, Cluster 2: 5139 CpGs). CpGs are further annotated according chromatin states defined in germinal center B cells and Kulis modules. (E) Box plots showing median DNA methylation levels of Cluster 1 (top) and Cluster 2 (bottom). bm-PC: plasma cells from bone marrow; HPC: hematopoietic stem cells; t-PC: plasma cells from tonsils.

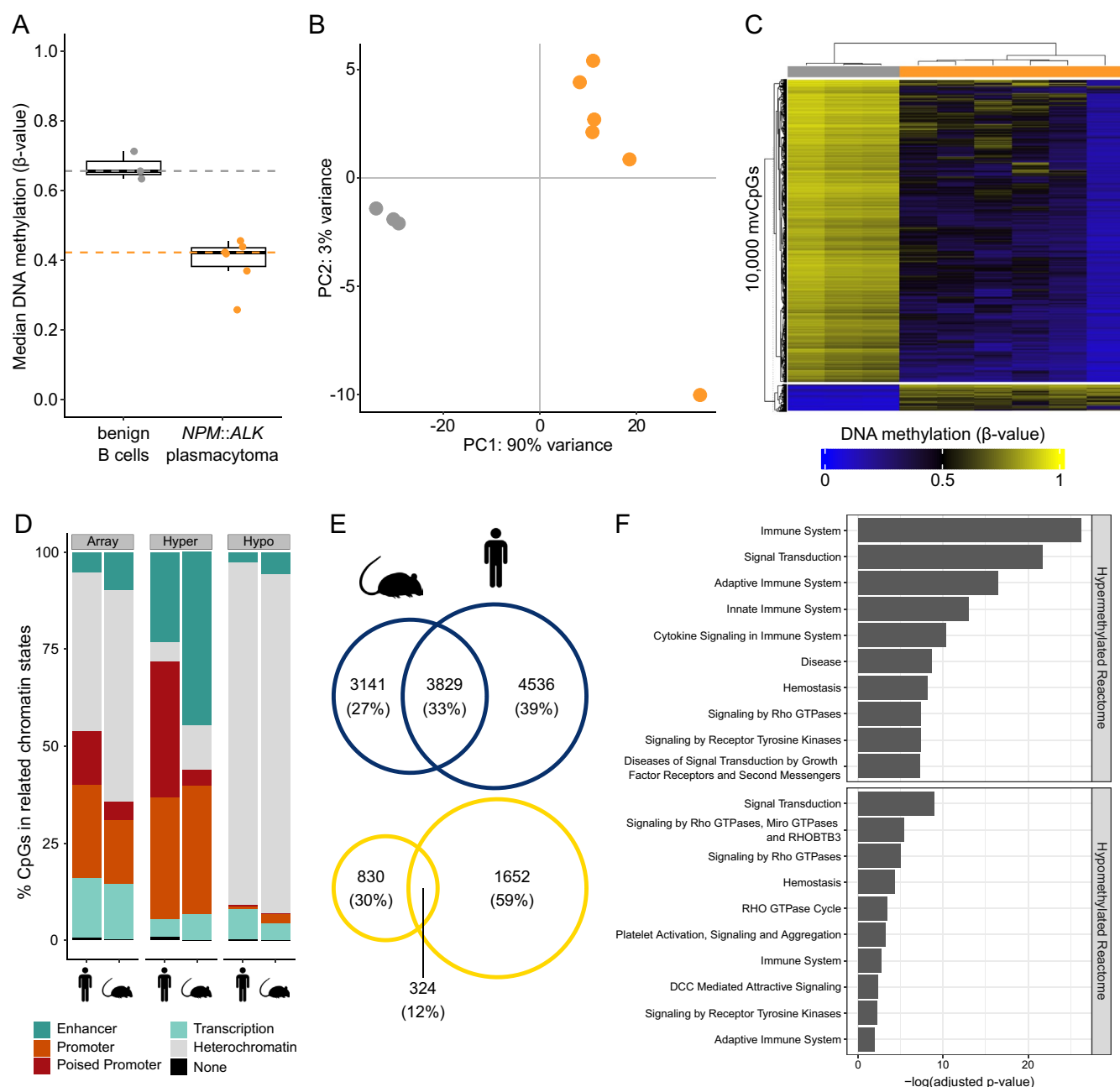


**FIGURE 2** | Comparative DNA methylation profiling of human and murine ALK-positive B-cell neoplasms. (A) Global median DNA methylation was calculated for *NPM::ALK* plasmacytoma and benign B cells (germinal center phenotype) from mice. (B) Principal component analysis of the murine samples based on the 10000 most variable CpGs. (C) Heatmap showing the DNA methylation levels of the 10000 most variable CpGs identified within the murine samples. (D) Chromatin state mapping of the significant differentially methylated CpGs found in human and murine ALK-positive B-cell neoplasms compared to their corresponding benign B cells (germinal center phenotype). As background comparison all CpGs entered the analysis were used (array: Human 441 770 CpGs; mouse 266 961 CpGs). Statistical analysis is summarized in Table S9. (E) Overlap of genes affected by differential DNA methylation in human and murine ALK-positive B-cell neoplasms (blue: Hypomethylation in tumor, yellow: Hypermethylation in tumor). (F) Gene ontology enrichment analysis (top ten according to adjusted  $p$  value) of hypermethylated and hypomethylated genes shared in human and murine with CpGs associated to regulatory regions (enhancer, promoter regions).

populations, reflecting the differentiation status of the tumor cells [11]. The most variable CpGs between ALK-positive LBCL, MM, and DLBCL distinctly separated ALK-positive LBCL from DLBCL, with a predominant hypomethylated phenotype associated with the Kulis module M9, which involves heterochromatin demethylation during late B-cell differentiation [14].

Despite the widespread use of transgenic and knock-out mouse models to study cancer biology, comparative DNA methylation studies between human and murine models driven by the same oncogene are limited [24, 25]. Taking advantage of the oncogenic driver potential of ALK-fusion in mouse and men, we here performed a cross-species comparison of B-cell neoplasms induced by ALK fusions in human and mouse samples [8]. Our

comparative findings show a conserved pattern of DNA methylation alterations in the ALK-driven B-cell tumors. Rather than at the single gene level, there seems to be functional conservation of the ALK-activation induced effects in malignant B cells, as can be seen from the common hypomethylation, the affected chromatin states, and the involved pathways jointly altered in both species. These findings not only highlight the relevance of the *NPM::ALK* mouse model for studying ALK-driven lymphomagenesis but also support the value of cross-species analyses in lymphoma research.

In summary, ALK-positive LBCL, both in humans and mice, shares epigenetic features with plasma cell neoplasms. Therefore, ALK-positive LBCL might be based on differentiation stage better grouped with plasma cell neoplasms rather than based on morphology as LBCL. Moreover, our findings showed conserved functional patterns between tumors induced by the same strong oncogenic driver in humans and corresponding mouse models, emphasizing the potential of cross-species DNA methylation profiling in both research and diagnostics.

### Author Contributions

A.L., S.K.H., A.D.Z., W.K., L.X., C.L., W.W., and S.M. provided human tumor samples and clinical data. C.V., R.C., S.S., and M.R. provided mouse samples and clinical data. S.B. performed and evaluated FISH studies. S.G., O.A., C.S.-M., and R.W. coordinated and analyzed DNA methylation data. R.S. and S.G. interpreted the data and wrote the manuscript. R.S. designed the study and coordinated the project. All authors read and approved the manuscript.

### Acknowledgments

This study has been supported by grants from the German Research Foundation (DFG) in the framework of the Collaborative Research Centres SFB 1074 and SFB 1530. We thank Life & Brain GmbH for providing the services of genome-wide DNA methylation profiling in mouse samples. We also thank Helene Kretzmer for her assistance with the segmentation of chromatin states, Laura Wiehle for coordinating the hybridization of samples, and the tumor genetic teams of the Institutes of Human Genetics in Kiel and Ulm for technical assistance and discussions. We acknowledge David Weinstock for his support in the generation of the patient-derived xenograft model. This work was supported by NIH/NCI R01 CA196703-01 to R.C. Open Access funding enabled and organized by Projekt DEAL.

### Ethics Statement

The study was approved by the Ethics Committee of the Medical Faculty of the Christian-Albrechts-University Kiel (D447/10, Amendment 2.11.2015).

### Consent

Written informed consent was obtained from the patients or their legal guardians in agreement with the regulations of the vote of the Ethic Committee of the Medical Faculty of the Christian-Albrechts University and the Institutional Review Boards of the involved institutions.

### Conflicts of Interest

The authors declare no conflicts of interest.

### Data Availability Statement

The data that support the findings of this study are openly available in Gene Expression Omnibus at <https://www.ncbi.nlm.nih.gov/geo/>, reference number GSE289985, GSE289988, and GSE289990.

### References

1. R. Alaggio, C. Amador, I. Anagnostopoulos, et al., "The 5th Edition of the World Health Organization Classification of Haematolymphoid Tumours: Lymphoid Neoplasms," *Leukemia* 36, no. 7 (2022): 1720–1748, <https://doi.org/10.1038/s41375-022-01620-2>.
2. J. J. Castillo, B. E. Beltran, L. Malpica, M. L. Marques-Piubelli, and R. N. Miranda, "Anaplastic Lymphoma Kinase-Positive Large B-Cell Lymphoma (ALK + LBCL): A Systematic Review of Clinicopathological Features and Management," *Leukemia & Lymphoma* 62, no. 12 (2021): 2845–2853, <https://doi.org/10.1080/10428194.2021.1941929>.
3. C. Laurent, C. Do, R. D. Gascoyne, et al., "Anaplastic Lymphoma Kinase-Positive Diffuse Large B-Cell Lymphoma: A Rare Clinicopathologic Entity With Poor Prognosis," *Journal of Clinical Oncology* 27, no. 25 (2009): 4211–4216, <https://doi.org/10.1200/JCO.2008.21.5020>.
4. L. Cerchietti, C. Damm-Welk, I. Vater, et al., "Inhibition of Anaplastic Lymphoma Kinase (ALK) Activity Provides a Therapeutic Approach for CLTC-ALK-Positive Human Diffuse Large B Cell Lymphomas," *PLoS One* 6, no. 4 (2011): e18436, <https://doi.org/10.1371/journal.pone.0018436>.
5. J. D. Soumerai, A. Rosenthal, S. Harkins, et al., "Next-Generation ALK Inhibitors Are Highly Active in ALK-Positive Large B-Cell Lymphoma," *Blood* 140, no. 16 (2022): 1822–1826, <https://doi.org/10.1182/blood.2022015443>.
6. D. Liu, L. Xing, H. Wang, P. Li, H. Wei, and Z. Li, "Case Report: A Patient With ALK-Positive Large B-Cell Lymphoma Benefited From Myeloma-Like Treatment Combined With the ALK Inhibitor Lorlatinib," *Frontiers in Hematology* 3 (2024): 1334577, <https://doi.org/10.3389/frhem.2024.1334577>.
7. S. W. Morris, M. N. Kirstein, M. B. Valentine, et al., "Fusion of a Kinase Gene, ALK, to a Nucleolar Protein Gene, NPM, in Non-Hodgkin's Lymphoma," *Science* 263, no. 5151 (1994): 1281–1284, <https://doi.org/10.1126/science.8122112>.
8. R. Chiarle, J. Z. Gong, I. Guasparri, et al., "NPM-ALK Transgenic Mice Spontaneously Develop T-Cell Lymphomas and Plasma Cell Tumors," *Blood* 101, no. 5 (2003): 1919–1927, <https://doi.org/10.1182/blood-2002-05-1343>.
9. K. Lange, W. Uckert, T. Blankenstein, et al., "Overexpression of NPM-ALK Induces Different Types of Malignant Lymphomas in IL-9 Transgenic Mice," *Oncogene* 22, no. 4 (2003): 517–527, <https://doi.org/10.1038/sj.onc.1206076>.
10. D. Hübschmann, K. Kleinheinz, R. Wagener, et al., "Mutational Mechanisms Shaping the Coding and Noncoding Genome of Germinal Center Derived B-Cell Lymphomas," *Leukemia* 35, no. 7 (2021): 2002–2016, <https://doi.org/10.1038/s41375-021-01251-z>.
11. X. Agirre, G. Castellano, M. Pascual, et al., "Whole-Epigenome Analysis in Multiple Myeloma Reveals DNA Hypermethylation of B Cell-Specific Enhancers," *Genome Research* 25, no. 4 (2015): 478–487, <https://doi.org/10.1101/gr.180240.114>.
12. M. R. Hassler, W. Pulverer, R. Lakshminarasimhan, et al., "Insights Into the Pathogenesis of Anaplastic Large-Cell Lymphoma Through Genome-Wide DNA Methylation Profiling," *Cell Reports* 17, no. 2 (2016): 596–608, <https://doi.org/10.1016/j.celrep.2016.09.018>.
13. S. T. Lee, Y. Xiao, M. O. Muench, et al., "A Global DNA Methylation and Gene Expression Analysis of Early Human B-Cell Development Reveals a Demethylation Signature and Transcription Factor Network," *Nucleic Acids Research* 40, no. 22 (2012): 11339–11351, <https://doi.org/10.1093/nar/gks957>.
14. M. Kulis, A. Merkel, S. Heath, et al., "Whole-Genome Fingerprint of the DNA Methylome During Human B Cell Differentiation," *Nature Genetics* 47, no. 7 (2015): 746–756, <https://doi.org/10.1038/ng.3291>.
15. C. C. Oakes, M. Seifert, Y. Assenov, et al., "DNA Methylation Dynamics During B Cell Maturation Underlie a Continuum of Disease

Phenotypes in Chronic Lymphocytic Leukemia,” *Nature Genetics* 48, no. 3 (2016): 253–264, <https://doi.org/10.1038/ng.3488>.

16. H. Kretzmer, S. H. Bernhart, W. Wang, et al., “DNA Methylome Analysis in Burkitt and Follicular Lymphomas Identifies Differentially Methylated Regions Linked to Somatic Mutation and Transcriptional Control,” *Nature Genetics* 47, no. 11 (2015): 1316–1325, <https://doi.org/10.1038/ng.3413>.

17. S. Sander, D. P. Calado, L. Srinivasan, et al., “Synergy Between PI3K Signaling and MYC in Burkitt Lymphomagenesis,” *Cancer Cell* 22, no. 2 (2012): 167–179, <https://doi.org/10.1016/j.ccr.2012.06.012>.

18. M. J. Aryee, A. E. Jaffe, H. Corrada-Bravo, et al., “Minfi: A Flexible and Comprehensive Bioconductor Package for the Analysis of Infinium DNA Methylation Microarrays,” *Bioinformatics* 30, no. 10 (2014): 1363–1369, <https://doi.org/10.1093/bioinformatics/btu049>.

19. Y. Luo, B. C. Hitz, I. Gabdank, et al., “New Developments on the Encyclopedia of DNA Elements (ENCODE) Data Portal,” *Nucleic Acids Research* 48, no. D1 (2020): D882–D889, <https://doi.org/10.1093/nar/gkz1062>.

20. M. E. Ritchie, B. Phipson, D. Wu, et al., “Limma Powers Differential Expression Analyses for RNA-Sequencing and Microarray Studies,” *Nucleic Acids Research* 43, no. 7 (2015): e47, <https://doi.org/10.1093/nar/gkv007>.

21. G. Delsol, L. Lamant, B. Mariamé, et al., “A New Subtype of Large B-Cell Lymphoma Expressing the ALK Kinase and Lacking the 2; 5 Translocation,” *Blood* 89, no. 5 (1997): 1483–1490.

22. R. D. Gascoyne, L. Lamant, J. I. Martin-Subero, et al., “ALK-Positive Diffuse Large B-Cell Lymphoma Is Associated With Clathrin-ALK Rearrangements: Report of 6 Cases,” *Blood* 102, no. 7 (2003): 2568–2573, <https://doi.org/10.1182/blood-2003-03-0786>.

23. U. Klein, S. Casola, G. Cattoretti, et al., “Transcription Factor IRF4 Controls Plasma Cell Differentiation and Class-Switch Recombination,” *Nature Immunology* 7, no. 7 (2006): 773–782, <https://doi.org/10.1038/ni1357>.

24. U. Lamprecht Tratar, S. Horvat, and M. Cemazar, “Transgenic Mouse Models in Cancer Research,” *Frontiers in Oncology* 8 (2018): 268, <https://doi.org/10.3389/fonc.2018.00268>.

25. A. Noguera-Castells, C. A. García-Prieto, G. Ferrer, et al., “A DNA Methylation Database of Human and Mouse Hematological Malignancy Cell Lines,” *Leukemia* 39, no. 2 (2024): 512–515, <https://doi.org/10.1038/s41375-024-02478-2>.

## Supporting Information

Additional supporting information can be found online in the Supporting Information section.